Electronic Supplementary Material (ESI) for Physical Chemistry Chemical Physics.


# Supporting information: Simulations of valence excited states in coordination complexes reached through hard x-ray scattering

Erik Källman,[†] Meiyuan Guo,[†] Mickaël G. Delcey,[†] Roland Lindh,[‡,¶] and Marcus Lundberg[*,†]

†*Department of Chemistry - Ångström Laboratory, Uppsala University, SE-751 20 Uppsala, Sweden*

‡*Department of Chemistry-BMC, Uppsala University, P.O. Box 576, SE-751 23 Uppsala*

¶*Uppsala Center for Computational Chemistry ($UC_3$), Uppsala University, P.O. Box 596, SE-751 24 Uppsala, Sweden*

E-mail: marcus.lundberg@kemi.uu.se

# Supporting Information Available

# List of Figures

# List of Tables

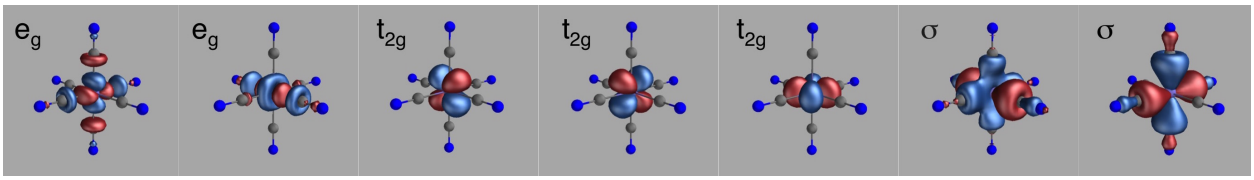


Figure 1: Isodensity representations of the seven orbitals in the RAS2 space. Orbital pictures are from the ferrocyanide ground state.

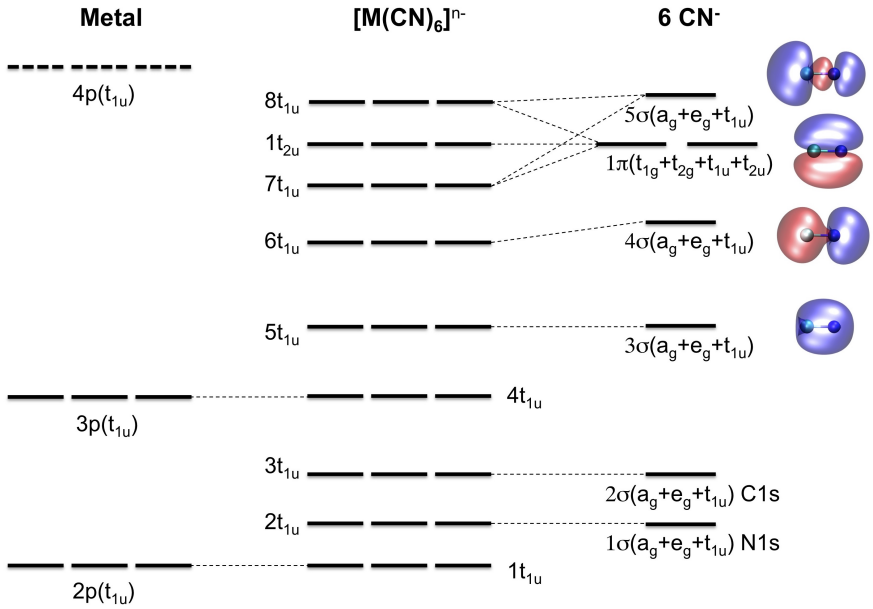


Figure 2: Orbital diagram of metal hexacyanides using the $O_h$ point group. Only orbitals in the $t_{1u}$ and $t_{2u}$ irreducible representations are included. Orbital energies are not to scale.

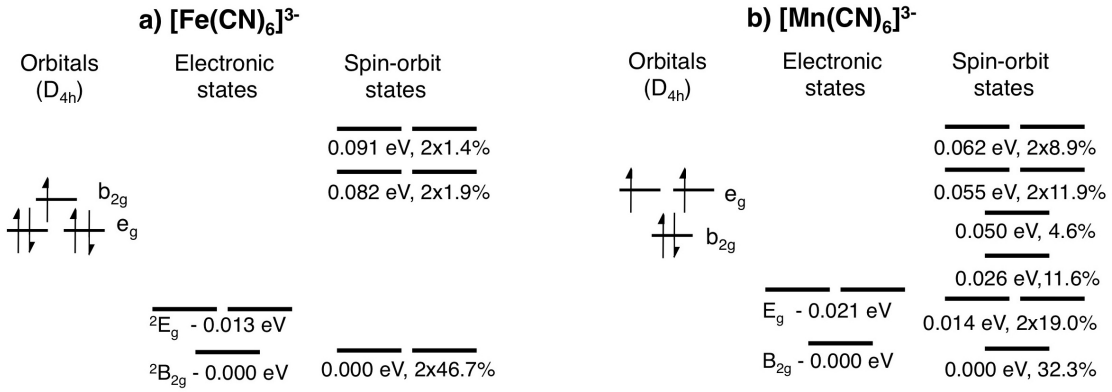


Figure 3: Low-lying states of ferri- and manganicyanide complexes calculated with RASPT2/RASSI. Energy diagrams are not to scale. Boltzmann populations of the spin-orbit states at 298.15 K are shown after the relative energies.

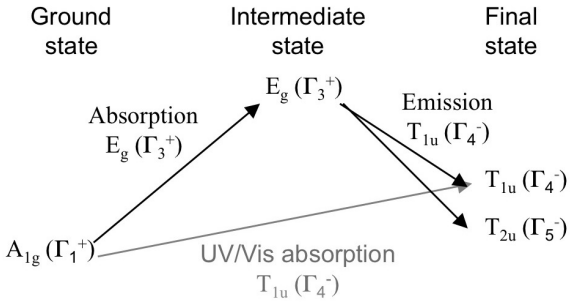


Figure 4: Selection rules for the valence RIXS process in ferrocyanide.

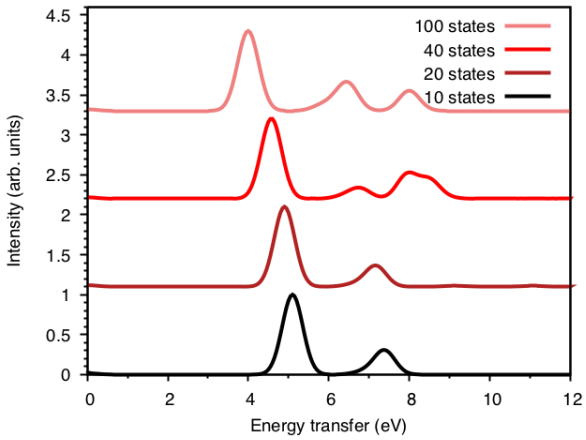


Figure 5: Constant incident energy cuts through the 7113.0 eV pre-edge peak of ferrocyanide using MS-RASPT2 and different number of ungerade valence states per irreducible representation.

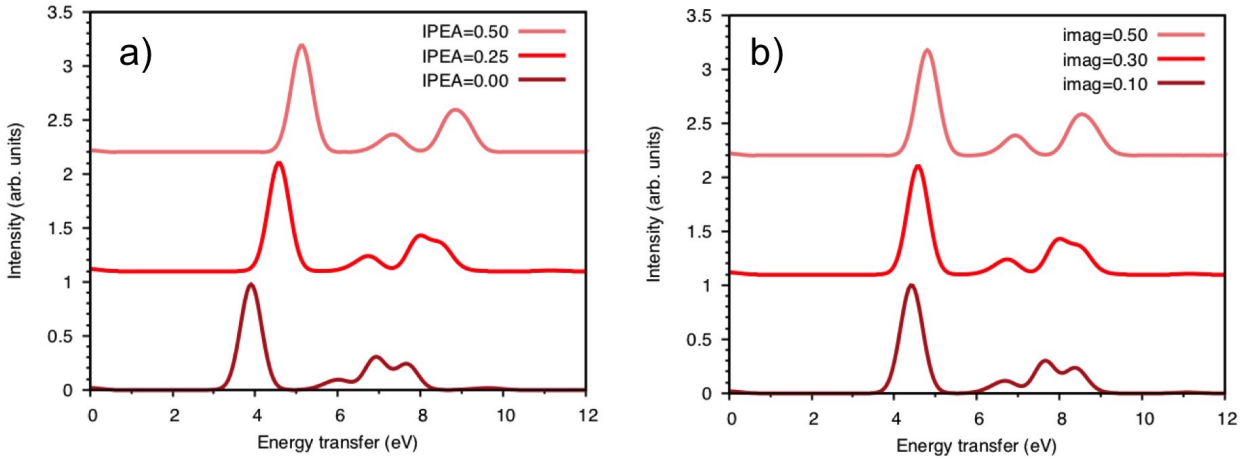


Figure 6: Constant incident energy cuts through the 7113.0 eV pre-edge peak of ferrocyanide using MS-RASPT2. a) Different values of the IPEA shift. b) Different values of the imaginary shift.

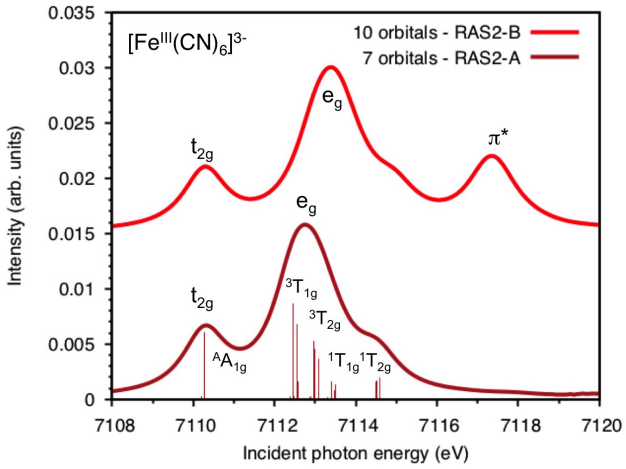


Figure 7: Metal K pre-edge XAS spectra of ferricyanide from MS-RASPT2 calculations with 60 core-excited states and different active spaces. Splittings between $t_{2g}$ and $e_g$ peaks increase by 0.50 eV when going from 7 to 10 gerade valence orbitals. All core-excited states are doublets. The labels for the different transitions correspond to the valence-electron configurations in the $d^6$ Tanabe-Sugano diagram as the exchange interactions with the 1s shell are small.

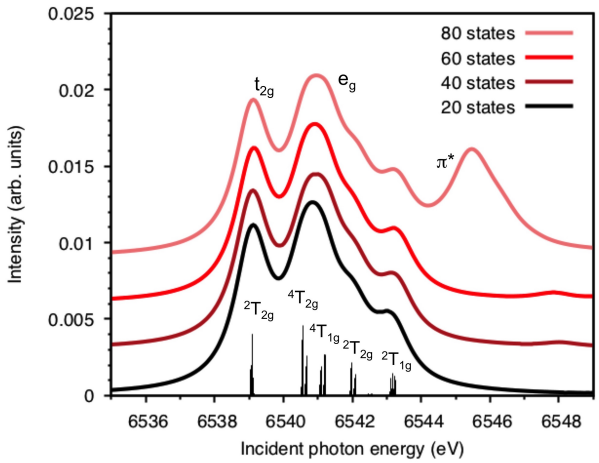


Figure 8: Metal K pre-edge XAS spectra of manganicyanide from MS-RASPT2 calculations using different number of core-excited states. Calculations have been performed with the 10-orbital RAS2-B active space. All core-excited states are triplets. The labels for the different transitions correspond to the main valence-electron configuration in the $d^5$ Tanabe-Sugano diagram as the exchange interactions with the 1s shell are small.

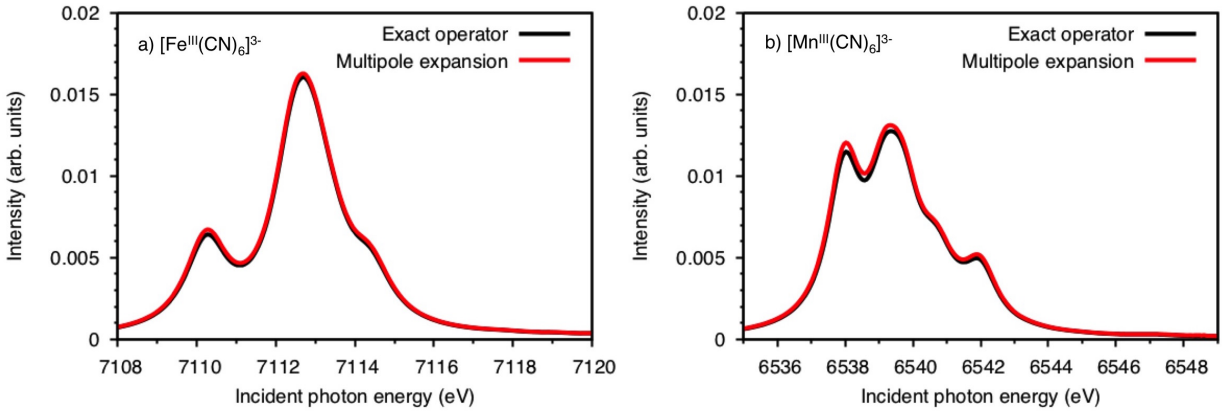


Figure 9: Metal K pre-edge XAS spectra of calculated using the second-order multipole expansion and the exact semi-classical form of the wave vector for a) ferricyanide and b) manganicyanide. Calculations have been performed with 60 core-excited states using the 7-orbital RAS2-A active space.

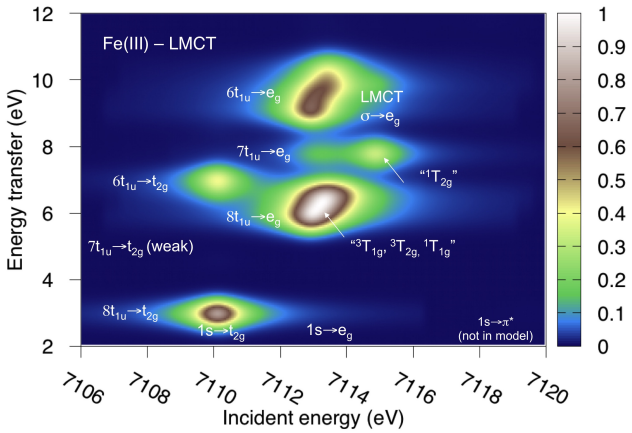


Figure 10: Metal K pre-edge RIXS spectra of ferricyanide from MS-RASPT2 calculations with 0.6 eV experimental broadening in the energy transfer direction.

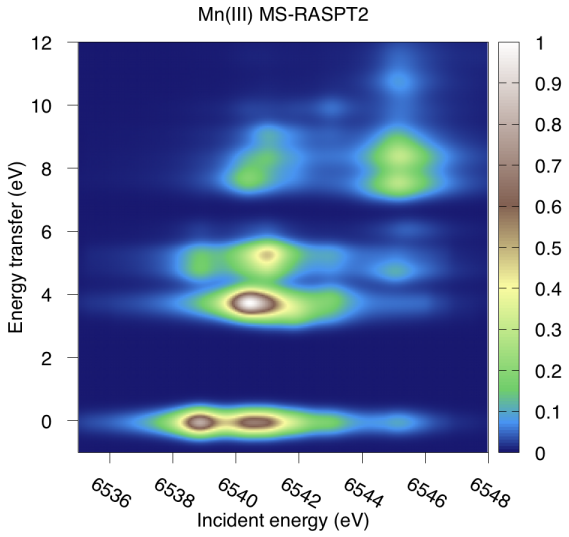


Figure 11: Metal-centered d-d excitations in the K pre-edge RIXS spectra of manganicyanide calculated using MS-RASPT2.

Table 1: Bond distances Å from RASPT2/ano-rcc-vtzp optimized geometries. Experimental distances are shown in parenthesis. The Jahn-Teller distorted geometries are $D_{4h}$. Other theoretical studies favor $D_{3d}$ over $D_{4h}$.[1,2] As the distortions are small the differences between these geometries should not affect the spectral simulations.[3]

| Distance | Mn(III) | Fe(III) | Fe(II) |
|---|---|---|---|
| M-C1 x 4 | 1.992 (2.013)[5] | 1.942 (1.94)[6] | 1.918 (1.913)[7] |
| M-C2 x 2 | 2.022 (2.023) | 1.921 (1.94) | 1.918 (1.913) |
| C1-N1 x 4 | 1.186 (1.161) | 1.184 (1.16) | 1.196 (1.161) |
| C2-N2 x 2 | 1.183 (1.156) | 1.186 (1.16) | 1.196 (1.161) |

Table 2: Number of states in each irreducible representation for calculations of ligand-to-metal charge-transfer spectra using 7 gerade valence orbitals in the active space (RAS2-A).

| Calculation | Symmetry | | | |
|---|---|---|---|---|
| $[Fe^{II}(CN)]_6 4-$ | $a_g$ | $b_{(1,2,3)g}$ | $a_u$ | $b_{(1,2,3)u}$ |
| Initial | 1 | 0 | 0 | 0 |
| Intermediate | 2 | 0 | 0 | 0 |
| Final | 0 | 0 | 2/6/10/20/40/60/100 | 2/6/10/20/40/60/100 |
| $[Fe^{III}(CN)]_6 3-$ | $a_g$ | $b_{(1,2,3)g}$ | $a_u$ | $b_{(1,2,3)u}$ |
| Initial | 0 | 1 | 0 | 0 |
| Intermediate | 60 | 60 | 0 | 0 |
| Final | 0 | 0 | 100 | 100 |
| $[Mn^{III}(CN)]_6 3-$ | $a_g$ | $b_{(1,2,3)g}$ | $a_u$ | $b_{(1,2,3)u}$ |
| Initial | 0 | 1 | 0 | 0 |
| Intermediate | 60 | 60 | 0 | 0 |
| Final | 0 | 0 | 100 | 100 |

Table 3: Number of states in each irreducible representation for calculations of metal-centered excitations using 10 gerade valence orbitals in the active space (RAS2-B).

| Calculation | Symmetry | | | |
|---|---|---|---|---|
| $[Fe^{III}(CN)_6]^{3-}$ | $a_g$ | $b_{(1,2,3)g}$ | $a_u$ | $b_{(1,2,3)u}$ |
| Valence | 60 | 60 | 0 | 0 |
| Core excited | 60 | 60 | 0 | 0 |
| $[Mn^{III}(CN)_6]^{3-}$ | $a_g$ | $b_{(1,2,3)g}$ | $a_u$ | $b_{(1,2,3)u}$ |
| Valence | 10/20/40/60/80 | 10/20/40/60/80 | 0 | 0 |
| Core excited | 10/20/40/60/80 | 10/20/40/60/80 | 0 | 0 |

Table 4: Incident energy shifts to align calculated spectra to first peak of the experimental K pre-edge spectra (7110.2 ev for $[Fe^{II}(CN)_6]^{4-}$, 7113.0 eV for $[Fe^{III}(CN)_6]^{3-}$, and 6539.1 eV for $[Mn^{III}(CN)_6]^{3-}$).

| Complex | RAS2 orbitals | Initial states | Core excited states | Shift (eV) |
|---|---|---|---|---|
| $[Fe^{II}(CN)_6]^{4-}$ | 7 | 1 | 2 | -19.25 |
| $[Fe^{III}(CN)_6]^{3-}$ | 7 | 1 | 60 | -18.99 |
| $[Fe^{III}(CN)_6]^{3-}$ | 10 | 60 | 60 | -19.57 |
| $[Mn^{III}(CN)_6]^{3-}$ | 7 | 1 | 60 | -13.92 |
| $[Mn^{III}(CN)_6]^{3-}$ | 10 | 10 | 10 | -15.30 |
| $[Mn^{III}(CN)_6]^{3-}$ | 10 | 20 | 20 | -15.28 |
| $[Mn^{III}(CN)_6]^{3-}$ | 10 | 40 | 40 | -15.44 |
| $[Mn^{III}(CN)_6]^{3-}$ | 10 | 60 | 60 | -15.28 |
| $[Mn^{III}(CN)_6]^{3-}$ | 10 | 80 | 80 | -15.03 |

Table 5: Transition dipole moments for 1s transitions ($T_{fi}$) and orbital compositions for the ground state of ferrocyanide calculated using RASSCF/ANO-RCC-VTZP. Orbital analysis performed using the Stout-Politzer method implemented in the MultiWfn program.[4]

| Basis function | $T_{fi}$ | $T_{fi}^2$ | Orbital composition (%) $8t_{1u}$ | $1t_{2u}$ | $7t_{1u}$ | $6t_{1u}$ |
|---|---|---|---|---|---|---|
| 2p | 2.57E-02 | 6.61E-04 | 0.002 | 0.000 | 0.003 | 0.002 |
| 3p | -7.45E-03 | 5.55E-05 | 0.793 | 0.000 | 1.482 | 0.943% |
| 4p | 2.17E-03 | 4.71E-06 | 0.094 | 0.000 | 0.785 | 0.154% |
| 5p | -7.39E-03 | 5.45E-05 | 0.059 | 0.000 | 0.000 | 0.017 |
| 6p | 5.78E-03 | 3.34E-05 | 0.031 | 0.000 | 0.000 | 0.012 |

# References


(1) Atanasov, M.; Comba, P.; Daul, C. A.; Hauser, A. DFT-Based Studies on the Jahn-Teller Effect in 3d Hexacyanometalates with Orbitally Degenerate Ground States. *J. Phys. Chem. A* **2007**, *111*, 9145–9163.

(2) Engel, N.; Bokarev, S. I.; Suljoti, E.; Garcia-Diez, R.; Lange, K. M.; Atak, K.; Golnak, R.; Kothe, A.; Dantz, M.; Kühn, O.; Aziz, E. F. Chemical bonding in aqueous ferrocyanide: experimental and theoretical X-ray spectroscopic study. *J. Phys. Chem. B* **2014**, *118*, 1555–1563.

(3) Pinjari, R. V.; Delcey, M. G.; Guo, M.; Odelius, M.; Lundberg, M. Cost and sensitivity of restricted active-space calculations of metal L-edge X-ray absorption spectra. *J. Comput. Chem.* **2016**, *37*, 477–486.

(4) Lu, T.; Chen, F. Multiwfn: A multifunctional wavefunction analyzer. *J. Comput. Chem.* **2012**, *33*, 580–592.

(5) Buschmann, W. E.; Liable-Sands, L.; Rheingold, A. L.; Miller, J. S. Structure and physical properties of hexacyanomanganate (III),[MnIII (CN) 6] 3-. *Inorganica Chim. Acta* **1999**, *284*, 175–179.

(6) Hocking, R. K.; Wasinger, E. C.; de Groot, F. M.; Hodgson, K. O.; Hedman, B.; Solomon, E. I. Fe L-edge XAS studies of $K_4[Fe(CN)_6]$ and $K_3[Fe(CN)_6]$: A direct probe of back-bonding. *J. Am. Chem. Soc.* **2006**, *128*, 10442–10451.

(7) Kuchar, J.; Černák, J.; Massa, W. Hydrate isomerism in [Cu(en)2(H2O)1.935]2[Fe(CN)6]·4H2O. *Acta Crystallogr. C* **2004**, *60*, m418–m420.